Antiferromagnetic coupling of Mn adsorbates to Fe(100)

J. Dresselhaus, D. Spanke, F. U. Hillebrecht, and E. Kisker
Institut für Angewandte Physik, Heinrich-Heine-Universität Düsseldorf, D-40225 Düsseldorf, Germany

G. van der Laan
Daresbury Laboratory, Warrington WA4 4AD, United Kingdom

J. B. Goedkoop and N. B. Brookes
European Synchrotron Radiation Facility, BP 220, F-38043 Grenoble Cedex, France
(Received 24 March 1997)

We investigate the magnetic properties of Mn adsorbates on Fe(100) in the regime up to a few monolayers. Magnetic circular dichroism in absorption shows long-range ferromagnetic order for the Mn adsorbate, with antiferromagnetic alignment with respect to the Fe substrate. Element-specific magnetic domain imaging and hysteresis measurements show that the macroscopic magnetic behavior of the Mn adlayer is fully determined by the Fe substrate. For coverages below 0.5 ML the Mn absorption spectra show rich structures that are typical for localized d states. From this the Mn ground state is identified as a mixture of atomiclike d^5 and d^6 states, with a local spin moment of $4.5\mu_B$. However, the circular dichroism is 2.4 times smaller than expected for this ground state, suggesting disorder within the Mn adsorbate with an ordered moment of $1.9\mu_B$ at 120 K. The magnetic signal vanishes near 1 ML coverage, consistent with the theoretically predicted $c(2\times2)$ antiferromagnetic ground state of the monolayer. [S0163-1829(97)04631-6]

The electronic and magnetic structure of transition-metal adlayers on ferromagnetic substrates is currently of interest for several reasons.[1] Numerous electronic structure calculations as well as experimental investigations have indicated that the reduction of coordination and/or dimensionality in thin films may strongly affect the electronic structure of the adsorbate, including the magnetic behavior.[2–7] In the extreme case this may lead to magnetic order in a material that in its bulk form does not shown magnetism.[6–10] Of particular interest are ultrathin Mn films and multilayers of Mn and the $3d$ transition metals, because the half-filled $3d$ shell of Mn may give rise to a large Mn moment, which does not occur in bulk Mn due to the antiferromagnetic ground state.[6–10] A fascinating aspect of the physics of Mn adsorbates on transition metals is the formation of two-dimensional ordered surface alloys at 1/2-ML coverage, which has been reported for Mn on Cu and Ni (001) surfaces.[11,12]

Previous experimental investigations of ultrathin Mn films include x-ray photoemission studies of the Mn $3s$ core level for Mn layers on Fe (Ref. 6) and Ag,[9] which were interpreted as evidence for a large Mn moment, although the degree of magnetic order could not be established. From spin-resolved electron-energy-loss spectroscopy on thicker deposits of Mn on Fe layers antiferromagnetism for Mn deposits of several layers was inferred.[13] By spin-resolved photoemission on the Mn $3p$ level, Roth *et al.*[14] found antiferromagnetic coupling between the Mn and the Fe magnetic moments for Mn layers with thickness up to 1 ML, and a disappearance of the magnetic signal above 1 ML. In contrast, for Mn on fcc Co and Ni, ferromagnetic coupling was found by magnetic circular dichroism.[12]

Theoretical investigations have been performed for an ideal monolayer or bilayer on Fe(100).[15–19] The influence of defects was addressed, e.g., by investigation of a vicinal surface.[20] These calculations have shown that various different magnetic configurations lead to stable solutions, which are very close in their total energy. This means that in a real experiment the magnetic structure may be modified by subtle differences, e.g., of temperature, lattice spacing, number, and nature of defects, etc. Considering only ferromagnetic order within the adsorbate layer [$p(1\times1)$ structure], a very sensitive dependence of the Mn magnetic order and moment on the exchange interaction between the Mn atoms was found,[15] changing from a low to a high spin configuration with increasing exchange interaction. For a large exchange interaction, both the parallel and antiparallel configurations have a moment of about $4\mu_B$. A low spin configuration only was obtained for antiferromagnetic coupling.[15,16] For an ideal interface, parallel coupling between Fe and Mn moments is the most stable one.[16,19] For thicker bct Mn layers on Fe, Bouarab *et al.*[16] find a tendency towards layered antiferromagnetism with ferromagnetic coupling with the Fe substrate, in agreement with the experimental findings for thicker Mn layers on Fe.[8,13] Recently, also nonferromagnetic spin arrangements within the adsorbate layer were considered.[17,18] For the monolayer a $c(2\times2)$ antiferromagnetic structure within the Mn layer with vanishing total Mn moment was found as the ground state. Elmousshine *et al.*[18] considered also $p(2\times2)$ ferrimagnetic structures with a net moment of about $1.6\mu_B$ either parallel or antiparallel to that of Fe. The parallel configuration was found to be only 15 meV in energy above the $c(2\times2)$ ground state, so that it is plausible that both configurations coexist in an experiment. Recently, calculations for surface impurities have been performed by Nonas *et al.*,[21] which are the most appropriate approach for coverages of less than a monolayer.

This rich variety of possible magnetic structures motivated us to study the magnetic behavior of Mn adsorbates on Fe(100) by magnetic circular dichroism in x-ray absorption as well as x-ray excited photoemission microscopy, in both cases measured via total yield. We observe a large dichroism opposite to that of Fe, indicating that the Mn deposit has

long-range ferromagnetic order aligned antiparallel to the magnetization in the Fe substrate. The experiments were carried out at the European Synchrotron Radiation Facility (ESRF) in Grenoble, France, on beamline 26, which is with circularly polarized radiation by a helical undulator (ID 12 B).[22] This type of undulator provides linear or right/left circular polarization by phasing the horizontal and vertical magnetic fields in the device.[22] The Dragon monochromator delivers a monochromatized beam of about 1 mm^2 cross section to the sample, with $\sim$400-meV energy spread under our operating conditions. The degree of circular polarization is $S_3 \approx 0.75$ at the Mn $2p$ threshold, and 0.85 at the Fe $2p$ edge. Photoabsorption was measured via total yield, while simultaneously monitoring the photon flux via the yield from an 800-nm Al foil in the beam behind the exit slit.

Fe surfaces were prepared by depositing 10 to 20 ML Fe onto a clean Ag (100) single-crystal surface. Fe and Mn were deposited under UHV conditions by electron beam heating from a rod (Fe) or from a W crucible (Mn). The growth of Mn on Fe is complicated by the differences in structure as well as the tendency for intermixing. In order to avoid segregation of Ag to the top of the Fe film, as well as to minimize interdiffusion of Mn and Fe deposition and subsequent measurements were carried out with the sample held at about 120 K. At this substrate temperature segregation of Ag to the top of the deposited Fe film is quenched.[23] The evaporation rates were determined by a quartz microbalance. The coverages are given in terms of monolayer equivalent, determined from the heights of the absorption edges. This led to small corrections of the coverages estimated from the deposition time combined with the rate. We estimate the precision to be $\pm 10\%$. The substrate was mounted such that the light was incident along a Fe(100) in-plane direction under 75° to the surface normal. The magnetic domain structure was determined by photoemission microscopy, employing an electrostatic instrument described by Engel *et al.*[24] (Staib PEEM 150). The microscope images the total yield onto a channelplate with fluorescent screen. The screen is viewed by a video camera, and images are recorded digitally in a microcomputer.[25]

For measuring hysteresis loops, a small field was applied using coils outside the vacuum chamber, while monitoring the total yield at the Fe or Mn $2p$ thresholds. No change of the total yield with applied field was detected using photon energies away from the absorption thresholds. Figure 1 shows a typical example for hysteresis loops obtained for 15-ML Fe covered by 0.5 ML of Mn, in this case prepared and measured at room temperature. The Fe loop shows a nearly rectangular shape typical for magnetization along an easy axis, in our case a (100) direction in the plane of the Fe epitaxial layer. For the thickness of our Fe film we do not expect an out-of-plane component of the magnetization.[26] The relatively small fields are sufficient to saturate the film magnetically, and the remanent magnetization is equal to the saturation magnetization. This is important for electron spectroscopic measurements performed on such films in the remanent state. Monitoring the total yield excited at the Mn $2p$ threshold yields the hysteresis loop for the Mn adlayer. It has the same shape as the loop for the substrate Fe film, however, it is inverted with respect to the Fe loop. This shows that the net magnetic moment in the Mn adlayer is oriented

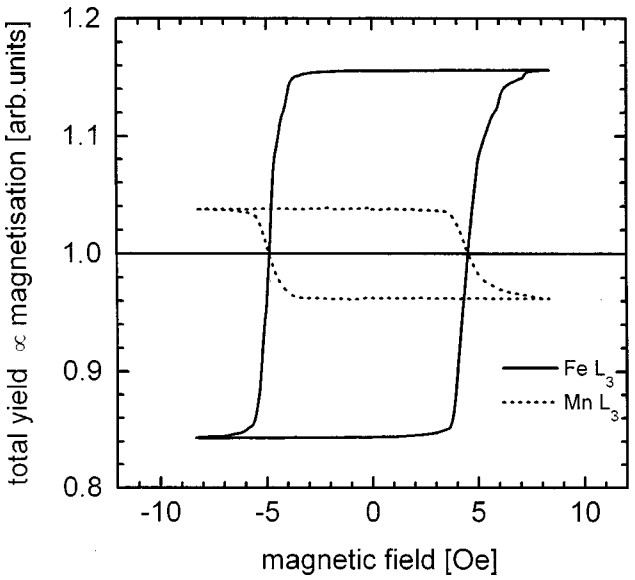

FIG. 1. Hysteresis loops for a nominal coverage of 0.5 ML Mn on 15 ML/Ag(100) prepared and measured at room temperature. Measurement by total yield at the Fe (full line) and Mn (dashed line) $2p_{3/2}$ thresholds. The vertical scale represents the total yield at the peak normalized to the average peak yield.

antiparallel to that in the Fe film (and to the external field). For a quantitative determination of magnetic moments it is important to note that the dichroism for the Mn adlayer saturates at the same magnetic field as the Fe dichroism.

Photoemission microscopy of films prepared at room temperature or at 120 K showed no magnetic contrast after they had been exposed to saturation field, confirming that they were single domain. In most cases, the films were a single domain immediately after preparation even without application of an external field. A multidomain state was generated by increasing the magnetic field until the total yield monitored simultaneously had changed to a value intermediate between the yield for two fully magnetized states, i.e., a field close to the coercive field. Photoemission micrographs revealing the magnetic domain structure for such a magnetization state are shown in Fig. 2 for 0.3-ML Mn deposited on 15-ML Fe at 120 K. The field of view in these micrographs is 320 μm. Usually, the magnetic contrast appears when one subtracts images taken with right- and left circular polarization. For our Fe surfaces the magnetic contrast is so large that it is visible and even dominates modulations of brightness caused by topographical effects. The different grey scales correspond to domains with different orientation of magnetization, the brightest and darkest corresponding to magnetization parallel and antiparallel to the incident light. The intermediate grey level represents a magnetization direction perpendicular to the incident light. In principle, the magnetization direction in this region can be determined by rotating the sample about its azimuth, however, this was not possible in our experiment. The micrograph shows 90° and 180° domain walls. From analysis of numerous micrographs we can say that for films in this very low thickness range 90° walls were much more abundant than 180° walls. Usually, these 90° domain boundaries run approximately but not exactly along (110) directions in the surface. The deviation from the (110) direction is possibly due to a small misorientation of the crystal surface. In some places these 90° domain

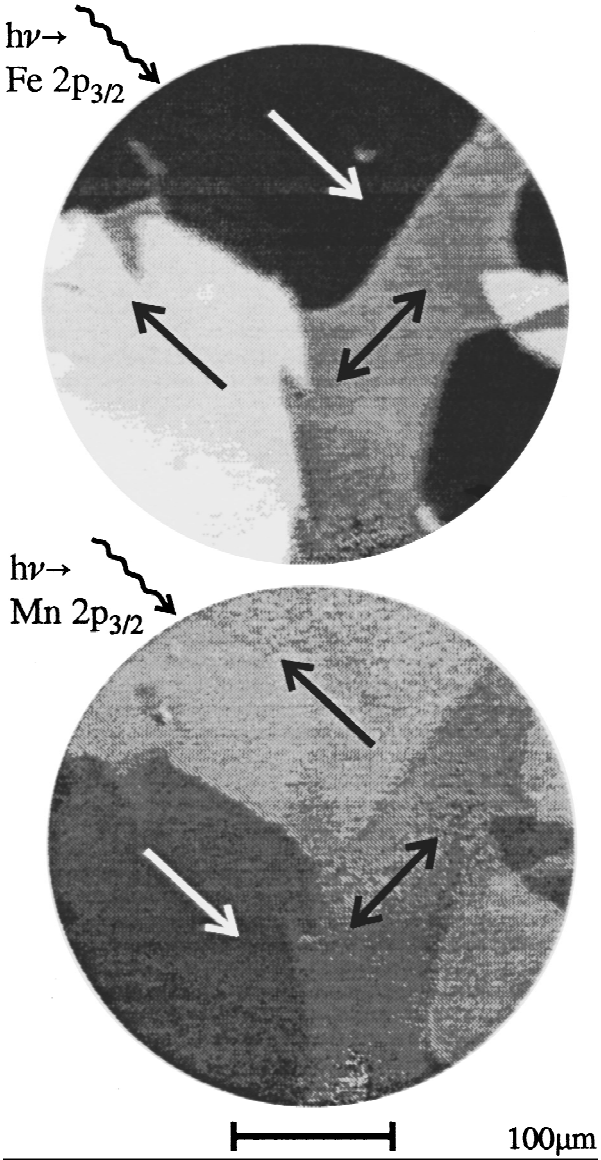

FIG. 2. Photoemission micrographs for 0.3 ML Mn/15 ML/Ag(100) grown at 120 K in the multidomain state. Images show subtraction of images taken with right- and left-circular radiation. Upper panel: magnetic contrast at the Fe $2p_{3/2}$ edge, $h\nu = 706$ eV. Lower: magnetic contrast at the Mn $2p_{3/2}$ edge, $h\nu = 638$ eV. Light incidence is indicated by the wavy arrow, which is close to a (100) direction in the surface. Arrows in the images indicate magnetization directions.

walls are decorated with sawtoothlike extensions. The contrast in the images is so large that a real-time measurement of the growth of a domain in a small magnetic field with a time resolution of 20 ms is possible.[27]

For circular dichroism measurements the films were exposed to saturation fields, so that they were single domain. The circular dichroism of the Fe film used as a substrate for Mn adsorption was measured before and after Mn adsorption. The $2p$ absorption spectrum of the pristine Fe film showed the well-known dichroism. The magnetic moment derived from application of the sum rule[28,29] was about $2.1\mu_B$ and $0.08\mu_B$ for the spin and orbital moments, respectively, using a d occupancy for Fe of $n_d = 7.4$. This result shows that the films are similar to bulk Fe.[28] For the lowest coverages considered here (up to 0.3 ML), the effect of Mn

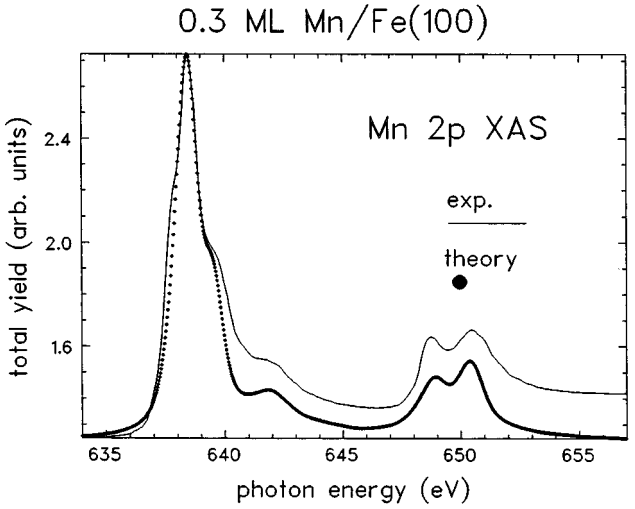

FIG. 3. Experimental (full line) and theoretical Mn $2p$ absorption spectra for 0.3 ML Mn on Fe, grown at 120 K. Spectra with σ^+ and σ^- light have been added. Dots show calculation for a mixed Mn d^5-d^6 atomic ground state as described in the text.

deposition at 120 K on the Fe magnetic dichroism was negligible. For higher coverages, the Fe dichroism shows a decrease of the Fe spin moment by 5–10% up to 2 ML of Mn, with an analogous decrease of the orbital moment. In contrast, Mn deposition with the substrate at room temperature quenches the Fe moment rapidly, indicating strong interdiffusion.

The Mn $2p$ absorption spectrum is shown in Fig. 3. It exhibits rich structure typical for localized systems. This ''isotropic'' spectrum, i.e., the spectrum averaged over both magnetizations, is similar to the calculation by van der Laan and Thole[30] for an atomic d^5 configuration. To derive quantitative information on the magnetic moment, we analyze the line shape in detail by comparing to a calculated spectrum. This avoids possible ambiguities connected with the sum rules, e.g., background subtraction, the number of d electrons, matrix elements, and the influence of the magnetic dipole term. Calculations were carried out on the basis of an atomic model.[31] The absorption spectrum was modeled by the transition $d^n \rightarrow 2p^5 3d^{n+1} \rightarrow 3d^{n-1} + \varepsilon$. The second step in this process, the Auger decay of the core hole, provides the linewidth in the calculated spectra. An additional Lorentzian broadening of 0.7 eV was included to account for all other broadening effects. To account for configuration-interaction effects, the Hartree-Fock values of the Slater integrals were reduced by 15%. When analyzing spectra of free atoms, a reduction by $20 \pm 10\%$ is usually needed to reproduce the observed peak positions; i.e., we are scaling the Slater integrals for the Mn adsorbate in a similar way as for free atoms. The quality of the fit indicates that the electronic structure of the Mn adsorbate on Fe(100) is not strongly influenced by interaction with the substrate, and justifies the treatment on the basis of an atomic model. Moreover, we found that the experimental spectrum is not satisfactorily described by considering a pure d^5 configuration as the initial state. A good agreement with the experimental spectrum is found when the ground state is described as a linear combination of d^5 and d^6 with weights 0.77 and 0.23, respectively. For both configurations only the Hund's rule ground states were considered. The spectrum calculated for this initial state

is shown in Fig. 3 together with the experimental spectrum. The spectra represent the sum of the spectra obtained for σ^+ and σ^- light. The agreement between experiment and theory is very good. The total spin moment for this mixed state is $4.55\mu_B$, which is smaller than the number of holes ($n_h = 4.77$) due to hybridization. This determination that is based purely on analyzing the *shape* of the absorption spectrum rather than applying the sum rules yields the *local* magnetic moment of the Mn adsorbate atoms, since it does not depend on the degree of magnetic order among these nearly atomlike magnetic moments.

The Mn XAS spectrum is very similar to that found for a dilute AgMn alloy,[32] for which also a large magnetic moment was derived from the spectrum. Theoretical calculations for Mn on the (100) surface of Ag, for a free-standing monolayer, or for an impurity in Ag (Refs. 2 and 5) yield a moment of the order of $4\mu_B$, in agreement with experimental findings.[32] Furthermore, the model spectra shown in Ref. 32 for different ground-state configurations demonstrate the sensitivity of the absorption spectrum to the local moment. Finally, we conclude from the large Mn moment that interdiffusion of Mn and Fe is not important, because then we would expect to find the moment characteristic for dilute Mn in Fe, which is of the order of $1\mu_B$,[33,34] aligned ferromagnetically with respect to Fe.

Figure 4 compares the experimental circular dichroism obtained for the same coverage to the Mn $2p$ absorption spectra for σ^+ and σ^- light calculated for the ground state described above. The experimental line shapes are quite different from the calculated ones, which apparently show a much larger dichroism. To compare the size of the dichroism, we subtract a constant signal equal to the level below threshold from the sum spectrum, and normalize the difference of the spectra for σ^+ and σ^- light to the maximum of the sum spectrum. The dichroism spectra obtained in this way are shown in the lowest panel of Fig. 4. The heights of the dichroism curves were normalized at the maximum. Surprisingly, there is very good agreement between experimental and theoretical circular dichroism in terms of the spectral *shape*, despite the discrepancy between the individual spectra. However, the *size* of the dichroism in experiment is 24% (taking the finite degree of circular polarization of 0.75 into account), while theory yields 58%; i.e., the experimental dichroism is 2.4 times smaller than in theory. This can be seen from the different scales for the experimental and theoretical spectra, as well as in the spectra calculated for right and left circular light shown in Fig. 4. The differences are strongest in the $j=\frac{3}{2}$region, where the experimental spectra show a single peak at the same photon energy for both helicities, while the calculation yields three peaks for one of the helicities, and essentially one peak with a shoulder for the other helicity. This shows that the experimental spectra for right and left circular radiation are a linear combination of spectra as calculated for completely oriented Mn atoms in the mixed d^5-d^6 ground state. This obviously leaves the sum (of right and left circular) spectrum as shown in Fig. 3 unaffected. It also leaves the dichroism spectrum unaffected except for a constant factor. From this analysis we obtain for the ordered moment, i.e., the projection of the Mn magnetic moment on the Fe magnetization direction, a value of $1.9\mu_B$.

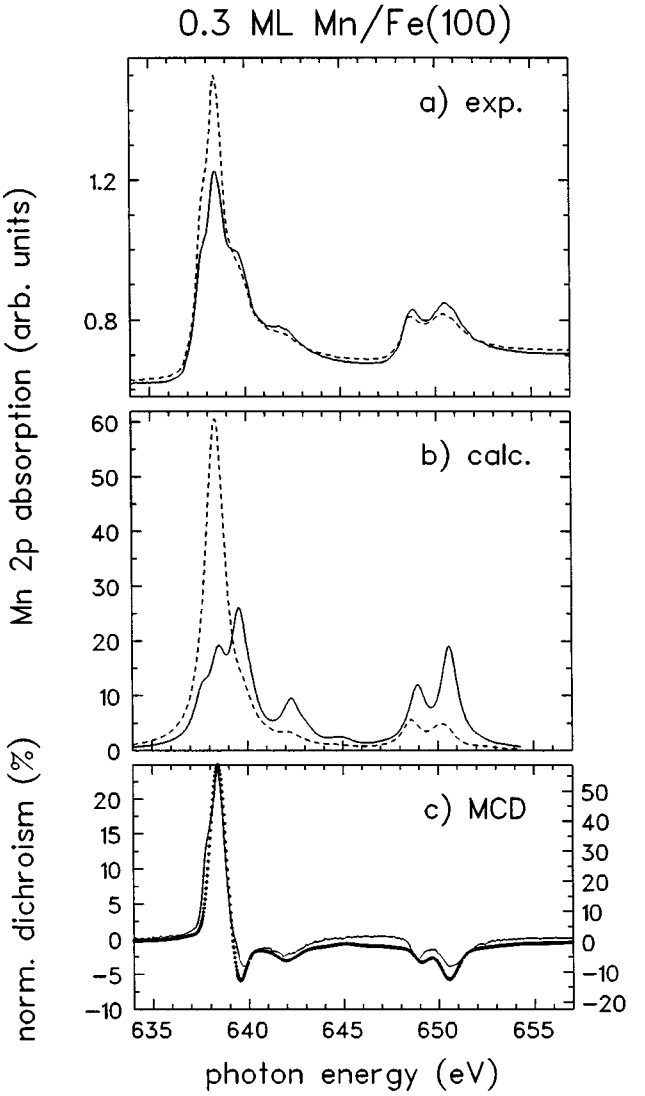

FIG. 4. Magnetic circular dichroism for 0.3 ML Mn on Fe(100): Experimental (a), as measured by total yield and calculated (b) spectra for σ^+ and σ^- light. (c) experimental (full line, left scale, divided by 0.75 to correct for 100% circular polarization) and calculated (dotted, right scale) magnetic circular dichroism.

The discrepancy between local and ordered magnetic moments may have different causes. The hysteresis measurement as well as our photoemission microscopy results rule out the presence of domains after applying magnetic fields above 10 Oe. Other possible reasons for the reduced magnetic signal are structural imperfections, spin canting, or temperature effects. If the small ordered moment is due to thermal fluctuations, one should see a dramatic increase of the magnetic moment at lower temperature. Our data at room temperature show a smaller Mn moment than at 120 K, however, this can also be caused by a change of the structural properties. Furthermore, as the net magnetic moment in the Mn adlayer is a result of the interaction with the Fe substrate, one would expect the ordered Mn magnetic moment to track the magnetization curve of Fe. If the spins are canted, i.e., not collinear with the Fe moments, one would observe a reduced magnetic moment in circular dichroism. A reduction as we observe here would indicate an angle between the Fe and Mn moments of 65°. This can be checked by using both helicities for each magnetization, so that one obtains an

MCD curve for each magnetization. If the Mn spins were oriented intermediate between perpendicular and in plane, then the two MCD signals would not be the same for oblique light incidence of 15°. However, our experiment yields the same Mn MCD for both magnetizations (also for Fe). This rules out a canting of the spins out of the surface plane (in the plane of Fe magnetization direction and the surface normal). A rotation of the Mn spins within the surface plane cannot be ruled out. If such an in-plane noncollinearity would be uniform on a macroscopic scale, such that the Mn moment would lie in the surface plane in a ferromagnetic ordering, but at some angle to the Fe magnetic moment, then one might expect to see this in the domain images. However, in all cases the Mn domain pattern was just the inversion of the Fe domain pattern. Finally, the hysteresis measurements show that the Mn moments saturate at the same field as the Fe moment, ruling out such a model.

For a submonolayer film, structural effects can arise from adsorption of the Mn at sites with different coordination, i.e., steps or kinks, or from clustering. Although we have no direct experimental evidence concerning the structural properties, the low temperature reduces the ability of the Mn atoms to migrate to steps, so that the Mn adatoms remain largely at the site of initial adsorption. The formation of monolayer patches, which according to theory[5,16,17] are antiferromagnetic and would not contribute to the magnetic signal, appears also unlikely for the same reasons, particularly for this low coverage. Also, for the full monolayer we observe a change of the spin-orbit branching ratio and other changes of the line shape, which show that the magnetic moment in the monolayer film is significantly smaller than for films below 0.5 ML. This is illustrated in Fig. 5, which shows a detail of the Mn $2p$ spectrum in the region of the $2p_{1/2}$ threshold for a number of coverages. One can clearly recognize that for the lowest coverages (0.15 and 0.3 ML) the $2p_{1/2}$ peak consists of two peaks separated by a minimum. As the coverage is increased above 0.5 ML, the minimum is filled up.

The similarity of our Mn spectrum for the adsorbate on Fe to that of dilute Mn in Ag (Ref. 32) suggests that the Mn atoms have very little interaction with other Mn atoms, or with the substrate. In principle, this is the situation in a dilute alloy, so that the electronic structure might show some analogies, keeping in mind that the reduced coordination of atoms adsorbed on the surface may affect the electronic structure due to reduced impurity host, or in our case, adatom-substrate interaction. However, dilute Mn/Fe alloys show quite different behavior[33,34] from the properties observed here, i.e., a magnetic moment of about $1\mu_B$ oriented parallel to the Fe moment. This is apparently due to the higher Mn/Fe coordination compared to a surface impurity. Recently a calculation for surface impurity atoms and surface dimers has been performed by Nonas *et al.*,[21] which is very illuminating for an understanding of our experimental results for the low coverages. In the calculation a true adatom as well as an Mn atom incorporated in the Fe surface layer (replacing an Fe atom) were considered. For both cases a magnetic moment of $3.4\mu_B$ was obtained. Interestingly, for the adatom a parallel (ferromagnetic) alignment with the substrate Fe was found, whereas for the Mn in the surface layer an antiparallel alignment was found. Mn is unique among the $3d$ transition metals inasfar as both the ferromagnetic and antiferromagnetic configurations lead to stable solutions. For a bcc (100) surface, the number of nearest Fe neighbors is the same (four) for the adatom and the surface atom, which may be the reason for the magnetic moments being similar. For the dimer, the ferromagnetic and ferrimagnetic solutions are found to be degenerate, with all the magnetic moments about $3.4\mu_B$. These results provide a plausible explanation for our experimental findings. The small ordered moment can be understood if we assume that the Mn atoms are residing on the surface as adatoms, as surface atoms, and as dimers. Since the moment is very similar in all these cases, the spectra of these differently coordinated Mn atoms will be very similar, and will be representative of a large magnetic moment. This corresponds to the large local moment observed in our experiment. However, the ordered moment is determined by how the Mn atoms are distributed between these different adsorption sites. The observed antiferromagnetic signal indicates that in our experiments the majority of atoms is incorporated in the Fe surface, since for this structure an antiferromagnetic coupling was found. Considering only these three structural configurations, between 40 (all remaining Mn atoms form dimers) and 70% (all remaining Mn atoms are in adatom sites) of the Mn atoms are estimated to be incorporated in the surface to give the antiferromagnetic signal. A similar process of atom exchange has been observed for Cr adsorbed on Fe(100) by scanning tunneling microscopy.[35]

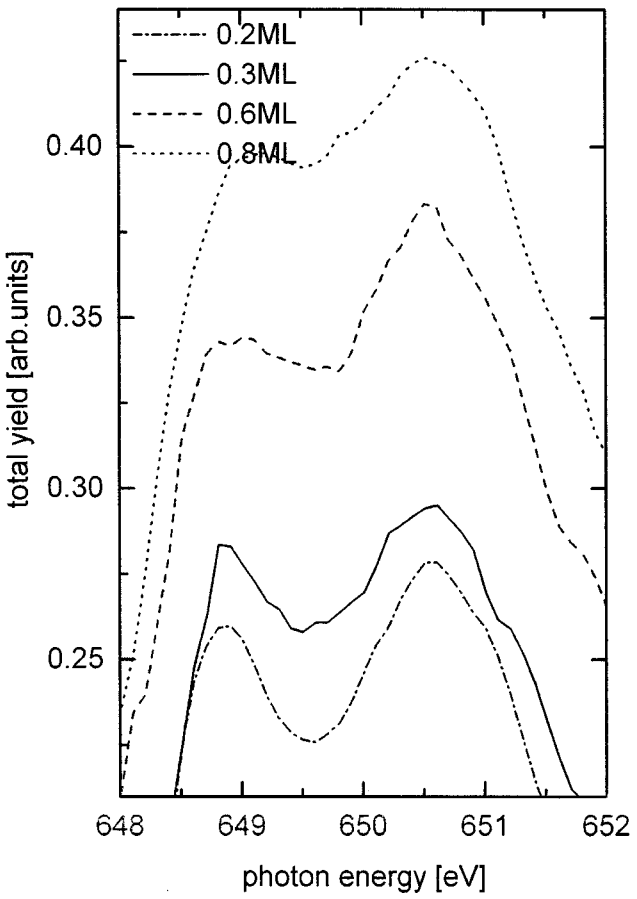

FIG. 5. Detail of the Mn $2p_{1/2}$ absorption spectra for different coverages of Mn on Fe(100) deposited at 120 K.

The size of the local moment determined here, $4.5\mu_B$, is somewhat larger than the moment obtained typically in vari-

ous calculations of Mn layers on Fe, or for surface impurities, which is about $3.5\mu_B$. To further clarify the origin of this discrepancy it is desirable to carry the electronic structure calculations further to obtain absorption spectra associated with a calculated electronic structure. Clearly, the spectrum for the buckled antiferromagnetic monolayer derived by Wu and Freeman[17] shows much less structure than the spectra observed here, even though the Mn moments are $3.1\mu_B$ and $-3.26\mu_B$ for the two different Mn sites.

The results presented here are in contrast to the results of Andrieu *et al.*[36] for adsorption of Mn on Fe(100), which indicated for the complete monolayer a ferromagnetic coupling of the Mn moments to the Fe substrate. Using the sum rule, a moment of $1\mu_B$ was determined for the monolayer. This experimental finding is in contrast to theoretical calculations, which consistently identify a $c(2\times2)$ antiferromagnetic or ferrimagnetic structure as the ground state of the monolayer, with very small dichroism signal.[5,17,18] The discrepancy in the sign of the coupling between the present results and those of Ref. 36 is not caused by the presence of Ag on our Fe surface in the present experiment, since the low substrate temperature quenches the diffusion of Ag to the top of the deposited Fe film. Furthermore, we have observed antiferromagnetic coupling for Mn/Fe/W (110) (Ref. 37) and for Mn/Fe/Cu (110) (Ref. 38) in the dilute (i.e., up to a monolayer) regime. Also, the spectra presented here (as well as those from our experiments on other surfaces) show much more structure than those in Ref. 36, which clearly suggests a larger moment in the present experiment. Possibly, different signs of the coupling are connected with different magnetic moments. More experiments are needed to clarify this issue.

We observe the same absorption spectrum and magnetic dichroism for 0.3 and 0.15 ML Mn coverage. This shows that within this coverage regime the structural and magnetic properties of the Mn adsorbate are essentially independent from coverage. For higher coverages, e.g., 0.6 ML, the Mn $2p$ absorption spectra change: the branching ratio decreases, and the minimum between the two $j=1/2$ features fills up (see Fig. 5). To illustrate the evolution of the shape of the spectrum towards that of bulk Mn, we show in Fig. 6 the branching ratio and the spin moment obtained from the Mn $2p$ spectra. One can clearly recognize the decrease of the branching ratio, which signals a decrease of the magnetic moment. This decrease is also found in the circular dichroism data. Since the spectra for higher coverages do not show structures as sharp as those in the lowest coverage regime, we now apply the sum rules to derive a relative measure for the change of spin moment with Mn coverage. The decrease of the magnetic moment is accompanied by a washing out of the fine structure of the atomic absorption spectrum. Nevertheless, even the spectrum for 15 ML shows still more structure than observed for bulk Mn.[37] The disappearance of the dichroism with increasing coverage can be ascribed to antiferromagnetic order within the Mn adlayer.

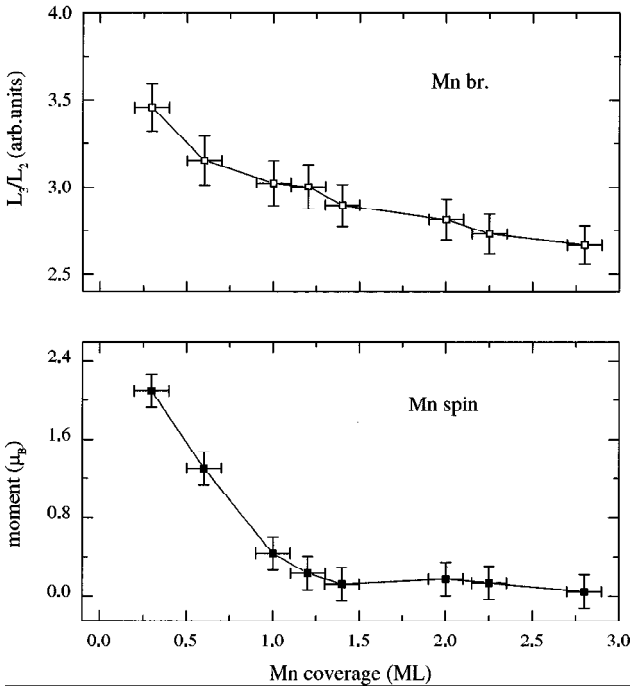

FIG. 6. Branching ratio (top) and spin moment (lower) as obtained by the sum rule for Mn $2p$ photoabsorption spectra as a function of Mn coverage on Fe(100).

In summary, we have shown by x-ray absorption spectroscopy that Mn adsorbates on Fe(100) have a local magnetic moment of $4.5\mu_B$. This result is derived from the line shape of the Mn absorption spectrum, without use of sum rules. This procedure is possible because the spectrum shows pronounced structure that is typical for systems with highly localized d electrons. Photoemission microscopy as well as element-specific hysteresis measurements demonstrate that the magnetic behaviour is fully determined by the Fe substrate. Magnetic circular dichroism shows that a 40% fraction of this moment is aligned antiparallel to the direction of the substrate Fe moments. The antiferromagnetic signal can be explained by the majority of Mn atoms being incorporated in the surface layer, whereas the reduced ordered moment shows that Mn atoms are also adsorbed as genuine adatoms or as dimers.

We thank J. Goulon, S. Ferte, L. Leclerc, and C. Troxel of the ESRF EXAFS group and P. Elleaume and J. Chavanne of the ESRF Insertion Device Group for their invaluable contributions to beamline 26. This work was supported by BMBF under Grant No. 05 644 PFA and by Deutsche Forschungsgemeinschaft (DFG) within SFB 166/G7.

[1] *Ultrathin Magnetic Structures*, edited by J. A. C. Bland and B. Heinrich (Springer, Berlin, 1994).

[2] C. Fu, A. J. Freeman, and T. Oguchi, Phys. Rev. Lett. **64**, 673 (1985).

[3] S. Blügel, B. Drittler, R. Zeller, and P. H. Dederichs, Appl. Phys. A **49**, 547 (1989); B. Drittler, N. Stefanou, S. Blügel, R. Zeller, and P. H. Dederichs, Phys. Rev. B **40**, 8203 (1989).

[4] O. Eriksson, R. C. Albers, and A. M. Boring, Phys. Rev. Lett. **66**, 1350 (1991).

[5] R. H. Victora and L. M. Falicov, Phys. Rev. B **31**, 7335 (1985).

[6] B. Heinrich, A. S. Arrott, C. Liu, and S. T. Purcell, J. Vac. Sci. Technol. A **5**, 1935 (1986).

[7] K. Takanashi, H. Yasuoka, N. Nakayama, T. Katamoto, and T. Shinjo, J. Phys. Soc. Jpn. **55**, 2357 (1986).
[8] S. T. Purcell, M. T. Johnson, N. W. E. McGee, R. Coehorn, and W. Hoving, Phys. Rev. B **45**, 13 064 (1992).
[9] D. A. Newstead, C. Norris, C. Binns, A. D. Johnson, and M.-G. Barthes, J. Phys. C **21**, 3777 (1986).
[10] B. T. Jonker, J. J. Krebs, and G. A. Prinz, Phys. Rev. B **39**, 1399 (1989).
[11] M. Wuttig, Y. Gauthier, and S. Blügel, Phys. Rev. Lett. **70**, 3619 (1993).
[12] W. L. O'Brien and B. P. Tonner, Phys. Rev. B **50**, 2963 (1994); **51**, 617 (1995).
[13] T. G. Walker and H. Hopster, Phys. Rev. B **48**, 3563 (1993).
[14] Ch. Roth, Th. Kleemann, F. U. Hillebrecht, and E. Kisker, Phys. Rev. B **52**, R15 691 (1995).
[15] M. A. Khan, S. Bouarab, H. Nait-Laziz, C. Demangeat, and M. Benakki, J. Magn. Magn. Mater. **148**, 76 (1995).
[16] S. Bouarab, H. Nait-Laziz, M. A. Khan, C. Demangeat, H. Dreyssé, and M. Benakki, Phys. Rev. B **52**, 10 127 (1995).
[17] Ruqian Wu and A. J. Freeman, Phys. Rev. B **51**, 17 131 (1995); J. Magn. Magn. Mater. **161**, 89 (1996).
[18] O. Elmouhssine, G. Moraitis, C. Demangeat, and J. C. Parlebas, Phys. Rev. B **55**, 7410 (1997).
[19] S. Mirbt, O. Eriksson, B. Johansson, and H. L. Skriver, Phys. Rev. B **52**, 15 070 (1995).
[20] O. Elmouhssine, M. Freyss, P. Krüger, J. C. Parlebas, C. Demangeat, J. Khalifeh, A. Vega, and A. Mokrani, J. Magn. Magn. Mater. **156**, 199 (1996).
[21] B. Nonas, K. Wildberger, R. Zeller, and P. H. Dederichs, J. Magn. Magn. Mater. **165**, 137 (1997).
[22] P. Elleaume, J. Synchrotron. Radiat. **1**, 19 (1994); N. B. Brookes and J. Goedkoop (unpublished).
[23] Due to the low substrate temperature one may expect rougher Fe surface obtained at room temperature, for which a reduced Fe moment was observed [J. A. C. Bland, R. D. Bateson, A. D. Johnson, B. Heinrich, Z. Celinski, and H. J. Lauter, J. Magn. Magn. Mater. **93**, 331 (1991)]. Despite the lower sample temperature, we observe the full Fe moment by circular dichroism. The quenching of Ag diffusion to the top of the deposited Fe film at reduced temperature was established by D. Bürgler *et al.* (unpublished).
[24] W. Engel, M. E. Kordesch, H. H. Rotermund, S. Kubala, and A. v. Oertzen, Ultramicroscopy **36**, 16 (1993).
[25] D. Spanke, Diploma thesis, Düsseldorf, 1995 (unpublished).
[26] Z. Q. Qiu, J. Pearson, and S. D. Bader, Phys. Rev. Lett. **70**, 1006 (1993).
[27] F. U. Hillebrecht, D. Spanke, J. Dresselhaus, and V. Solinus, J. Electron Spectrosc. Relat. Phenom. (to be published).
[28] B. T. Thole, P. Carra, F. Sette, and G. van der Laan, Phys. Rev. Lett. **68**, 1943 (1992); P. Carra, B. T. Thole, M. Altarelli, and X. Wang, *ibid.* **70**, 694 (1993).
[29] C. T. Chen, Y. U. Idzerda, H.-J. Lin, N. V. Smith, G. Meigs, E. Chaban, G. H. Ho, E. Pellegrin, and F. Sette, Phys. Rev. Lett. **75**, 152 (1995).
[30] G. van der Laan and B. T. Thole, Phys. Rev. B **43**, 13 401 (1991).
[31] B. T. Thole, G. van der Laan, and M. Fabrizio, Phys. Rev. B **50**, 11 466 (1994).
[32] B. T. Thole, R. D. Cowan, G. A. Sawatzky, J. Fink, and J. C. Fuggle, Phys. Rev. B **31**, 6856 (1985).
[33] M. F. Collins and G. G. Low, Proc. R. Soc. London, Ser. A **86**, 535 (1965).
[34] P. Radhakrishna and F. Livet, Solid State Commun. **25**, 597 (1978).
[35] A. Davies, J. A. Stroscio, D. T. Pierce, and R. J. Celotta, Phys. Rev. Lett. **76**, 175 (1996).
[36] S. Andrieu, M. Finazzi, F. Yubero, H. Fischer, P. Arcade, F. Chevrier, K. Hricovini, G. Krill, and M. Piecuch, J. Magn. Magn. Mater. **165**, 191 (1997).
[37] D. Spanke *et al.* (unpublished).
[38] H. A. Dürr, G. van der Laan, D. Spanke, F. U. Hillebrecht, N. B. Brookes, and J. B. Goedkoop, Surf. Sci. **377-379**, 466 (1997).